Interferon regulatory factor-4 activates IL-2 and IL-4 promoters in cooperation with c-Rel

Hisakazu Shindo[†, 1, 3], Kiyoshi Yasui[†, 1], Kazuo Yamamoto[1, 5], Kiri Honma[2], Katsuyuki Yui[2], Tomoko Kohno[1], Yuhua Ma[1], Koon Jiew Chua[1], Yoshinao Kubo[1], Hitoshi Aihara[4], Takashi Ito[4], Takeshi Nagayasu[3], Toshifumi Matsuyama[1,*], Hideki Hayashi [1]

([†]both authors contributed equally to this work)

[1]Division of Cytokine Signaling, and [2]Division of Immunology, Department of Molecular Microbiology and Immunology, [3]Division of Surgical Oncology, Department of Translational Medical Sciences, and [4]Department of Biochemistry, Nagasaki University Graduate School of Biomedical Sciences, 1-12-4 Sakamoto, Nagasaki 852-8523, Japan, and [5]University of Toronto, Toronto, Ontario, Canada.

Correspondence: Toshifumi Matsuyama, M.D., Ph.D.

Division of Cytokine Signaling, Department of Molecular Microbiology and Immunology, Nagasaki University Graduate School of Biomedical Sciences, 1-12-4 Sakamoto, Nagasaki 852-8523, Japan

Phone and Fax: +81-95-849-7001

E-mail: tosim@nagasaki-u.ac.jp

Abstract

Interferon regulatory factor (IRF)-4 is a member of the IRF transcription factor family, whose expression is primarily restricted to lymphoid and myeloid cells. In T-cells, IRF-4 expression is induced by T-cell receptor (TCR) cross-linking or treatment with phorbol-12-myristate-13-acetate (PMA)/Ionomycin, and IRF-4 is thought to be a critical factor for various functions of T-cells. To elucidate the IRF-4 functions in human adult T-cell leukemia virus type 1 (HTLV-1)-infected T-cells, which constitutively express IRF-4, we isolated IRF-4-binding proteins from T-cells, using a tandem affinity purification (TAP)-mass spectrometry strategy. Fourteen proteins were identified in the IRF-4-binding complex, including endogenous IRF-4 and the nuclear factor-kappaB (NF-κB) family member, c-Rel. The specific association of IRF-4 with c-Rel was confirmed by immunoprecipitation experiments, and IRF-4 was shown to enhance the c-Rel-dependent binding and activation of the interleukin-4 (IL-4) promoter region. We also demonstrated that IL-2 production was also enhanced by exogenously-expressed IRF-4 and c-Rel in the presence of P/I, in T-cells, and that the optimal IL-2 and IL-4 productions *in vivo* was IRF-4-dependent using IRF-$4^{-/-}$ mice. These data provide molecular evidence to support the clinical observation that elevated expression of c-Rel and IRF-4 is associated with the prognosis in adult T-cell leukemia/lymphoma (ATLL) patients, and present possible targets for future gene therapy.

Research Highlights

● Interferon regulatory factor-4 binds to an NF-kappaB family member, c-Rel, in T cells.

● The N-terminal half of c-Rel bound to the C-terminal IRF association domain of IRF-4.

● IRF-4 and c-Rel bound to the interleukin-4 (IL-4) promoter region.

● Exogenously-expressed IRF-4 and c-Rel enhanced the IL-2 production in T-cells.

● IRF-4 was indispensable for the optimal IL-2 and IL-4 productions in vivo.

Keywords

Interferon regulatory factor (IRF)-4; c-Rel; IL-4; IL-2; adult T-cell leukemia/lymphoma (ATLL).

Abbreviations

IRF-4, interferon regulatory factor-4; IFN, interferon; ISRE, IFN-stimulated response element; TCR, T-cell receptor; PMA, phorbol-12-myristate-13-acetate; I, Ionomycin; TAP, tandem affinity purification; IL-4, interleukin-4; HTLV-1, human adult T-cell leukemia virus type 1; ATLL, adult T-cell leukemia/lymphoma; NF-κB, nuclear factor-kappaB; NFATc2 (NFAT1), nuclear factor of activated T-cells; AZT, azidothymidine (zidovudine).

1. Introduction

Interferons (IFNs) are multi-functional cytokines that regulate the genes involved in viral infection defense, immune system activation, hematopoietic development and modulation of cell growth. IFNs derive their effects through the transcriptional activation of target genes, which are regulated through IFN regulatory factors (IRFs). In mammals, the members of the IRF family of transcription factors (IRF-1~IRF-9) bind to the IFN-stimulated response elements (ISREs) found in the promoter regions of IFN-stimulated genes (1).

The expression of IRF-4 is restricted to the immune system, and is induced by diverse mitogenic stimuli, including T-cell receptor (TCR) cross-linking or treatment with phorbol-12-myristate-13-acetate (PMA)/Ionomycin (I) (2-4). Mice deficient in the IRF-4 gene (IRF-$4^{-/-}$) exhibited profound defects in the functions of both B- and T-cells (5). IRF-4 plays crucial roles in multiple steps of B-cell differentiation. For instance, IRF-4 activates the immunoglobulin light-chain genes by binding a specific DNA sequence in the 3' enhancer regions, in cooperation with the ETS-family transcription factor PU.1, and by repressing the key germinal center regulator, BCL6 (6,7). Recently, IRF-4 was reported to be the master regulator gene in multiple myeloma, a malignancy of plasma cells (7,8). IRF-4 is also essential for several stages of T-cell and myeloid cell differentiation. We, as well as other groups, have found that, in the absence of IRF-4, not only the development of Th2 but also that of a cDC subset, $CD8\alpha^{-}CD11b^{+}$, is severely impaired (9-12). The IRF-4 functions are regulated by several IRF-4-binding proteins. FK506-binding protein 52 (FKBP52) reportedly bound to IRF-4 in HTLV-1 (human T-cell leukemia virus type 1)-infected T-cells, and repressed the IRF-4 function by preventing the nuclear translocation

and the target DNA binding of IRF-4 (13). The IRF-4-dependent IL-4 induction in the presence of PMA and Ionomycin was enhanced by NFATc2 (NFAT1), and provided an important molecular function in T-helper cell (Th) differentiation (9). NFATc1 (NFAT2) also activated the human IL-2 and IL-4 promoters in cooperation with IRF-4 (14). Recently, it was reported that the elevated expressions of a nuclear factor-kappaB (NF-κB) family member, c-Rel, and IRF-4 are associated with the prognosis in adult T-cell leukemia/lymphoma (ATLL) patients (15). To elucidate the mechanism, we isolated IRF-4-binding proteins from the HTLV-1-infected T-cells (HUT102), using the tandem affinity purification (TAP) method (16). We identified c-Rel, as a novel IRF-4-associated protein in T-cells. We further examined whether IRF-4 activates the promoters of IL-2 (a T-cell growth factor) and IL-4 (an inducer of Th2 differentiation and growth) in cooperation with c-Rel in the stimulated T-cells.

2. Materials and Methods

2.1. Cell culture and transfection

HUT102, an HTLV-1-infected human T-cell line, and EL-4, a murine thymoma cell line, were grown in RPMI 1640 medium supplemented with 10% heat-inactivated fetal bovine serum (FBS), and transfected with the indicated plasmids by electroporation using a pipette-type electroporator, Microporator MP-100 (Digital Bio). HEK293T cells were grown in 10% FBS-supplemented DMEM, and transfected with the indicated plasmids using the FuGENE 6 transfection reagent (Roche).

2.2. Plasmid constructs

The full-length human IRF-4 cDNA (1-1356) (2), and the PCR-amplified DNA fragments, (1-405) and (404-1356), were inserted downstream of the FLAG tag in the pcDNA3 vector (Invitrogen). The unique restriction enzyme, ApaI, was used to excise the N-terminal (1-1174) and C-terminal (1174-1860) regions from the full-length human c-Rel cDNA (1-1860)(17). The fragments were inserted downstream of the HA tag in the pcDNA3 vector. The IL-4-Luc reporter plasmid was constructed by inserting the PCR-amplified promoter region (-250 ~ +15) of the human IL-4 gene into the pGL2-Basic vector (Promega). All constructs were confirmed by DNA sequencing.

2.3. Preparation of cell extracts

Cell lysates were prepared by vigorous vortexing in 400 μl of lysis buffer (20 mM Tris, pH 8.0, 150 mM NaCl, 1 mM EDTA, 1% NP40), containing a protease inhibitor mix (Boehringer), 48 hour after transfection in a 6-well plate.

For the preparation of the nuclear extract, HUT102 cells (1×10^6 cells) were transfected with the indicated plasmids, and the nuclear proteins were extracted as described

previously (18).

2.4. Immunoprecipitation and immunoblot analyses

The cell lysates were incubated with anti-FLAG M1 antibody-conjugated agarose beads (Sigma) for 2h at 4°C. The nuclear extracts from HUT102 cells were incubated with 5μg of goat polyclonal anti-IRF-4 antibody (Santa Cruz Biotechnology), rabbit polyclonal anti-c-Rel antibody (Santa Cruz Biotechnology) or the corresponding control IgG antibody (Sigma), and Protein A Sepharose4B Fast Flow beads, for 3h at 4°C. The immunocomplexes were extensively washed, and the co-precipitated proteins were eluted from the Sepharose beads by boiling in SDS sample buffer. Each sample was resolved by SDS-PAGE, transferred to a PVDF membrane, and incubated with the indicated antibodies. Specific proteins were visualized with the appropriate HRP-conjugated antibodies and the ECL Plus detection system (Amersham Pharmacia Biotech).

2.5. Chromatin immunoprecipitation (ChIP)

The nuclear extracts from HUT102 cells were subjected to DNA-protein cross-linking with 1% formaldehyde for 5min. After extensive washing, the samples were suspended in 500 μl of 150 mM NaCl, 25 mM Tris, pH 7.5, 5 mM EDTA, 1% Triton X-100, 0.1% SDS, and 0.5% deoxycholate, and were sonicated. After centrifugation at 14,000 rpm for 10 min at 4°C, the supernatants were precipitated with 25 μg anti-IRF-4 antibody, anti-c-Rel antibody, or the corresponding IgG (Sigma) (as a control), and Protein A Sepharose4B Fast Flow beads. The amounts of precipitated DNA were quantified by PCR, using a pair of IL4 promoter-specific primers (Forward: 5'-CAAAGCAAAAAGCCAGCA-3', Reverse: 5'-CGTTACACCAGATTGTCAGTCAC-3').

2.6. Mice and primary T-cell activation

IRF-4 deficient (IRF-$4^{-/-}$) mice were initially mated to C57BL/6 mice, and were maintained by intercrossing in the Laboratory Animal Center for Animal Research at Nagasaki University. Mice were used at 5–6 weeks of age. The animal experiments reported herein were conducted according to the Guidelines of the Laboratory Animal Center for Biomedical Research at Nagasaki University.

Freshly isolated $CD4^+$ T-cells, from the spleens of C57BL/6 and IRF-$4^{-/-}$ littermates, were treated continuously with TNF-α (5 ng/ml) for 6h. The cells were then collected by centrifugation and cultured at a density of 1×10^6 cells/ml in six-well plates precoated with anti-TCRβ mAb (H57-597, 10 μg/ml). Cells were harvested at 4h for RNA analyses.

2.7. RNA isolation and reverse-transcription PCR

Total RNA was extracted from the $CD4^+$ T-cells and the HUT102 cells transfected with the indicated plasmids, using Isogen (Nippon Gene, Japan). cDNA was generated from 1 μg RNA, using reverse transcriptase. The PCR primers used for human IL-2 were 5'-TGTACAGCATGCAGCTCGC-3' and 5'-TGCTTCCGCTGTAGAGCTTG-3', those for mouse IL-2 were 5'-GAGTCAAATCCAGAAGATGCCGCAG -3' and 5'-TGATGGACCTACAGGAGCTCCTGAG-3', those for mouse IL-4 were 5'-CGAAGAACACCACAGAGAGTGAGCT-3' and 5'-GACTCATTCATGGTGCAGCTTATCG-3', those for G3PDH were 5'-CATCTGAGGGCCCACTGAAG-3' and 5'-TGCTGTTGAAGTCGCAGGAG-3', those for human β-actin were 5'-AAGAGAGGCATCCTCACCCT-3' and 5'-TACATGGCTGGGGTGTTGAA-3, and those for mouse β-actin were 5'-TGGAATCCTGTGGCATCCATGAAAC-3' and

5'-TAAAACGCAGCTCAGTAACAGTCCG-3'.

Intraperitoneal injections and cell isolation

Complete and incomplete Freund's adjuvants (CFA/IFA) were purchased from Difco Laboratories. An emulsion (100 μl) of CFA in PBS was injected into each of the C57BL/6 and IRF-$4^{-/-}$ littermates, followed by an injection of 100 μl of IFA on the next day. PBS alone was used as a negative control for all experiments. The animals were sacrificed on day 6. Lymphocytes were collected from the spleens. Total $CD4^+$ T-cells were purified using magnetic particles conjugated with anti-CD4 Ab (Imag Cell Separation System, BD Biosciences), as specified by the manufacturer. This protocol provided cells with >99% purity, as assessed by flow cytometry. Freshly isolated $CD4^+$ T-cells were collected by centrifugation and cultured at a density of 1×10^6 cells/ml in six-well plates precoated with various concentrations of anti-TCRβ mAb (H57-597). Cells were harvested at 16 h for cytokine assays, using sandwich ELISA. For the mRNA preparation, the isolated $CD4^+$ T-cells (2×10^5 cells/well) were stimulated in the 96-well paltes precoated with the indicated concentrations of anti-CD3 (Pharmingen) and anti-CD28 (Southern Biotech) antibodies for 4h.

3. Results

3.1. Identification of the proteins associated with IRF-4 by the TAP method, followed by mass spectrometry

To identify the proteins that associate with IRF-4 in T-cells, we purified the IRF-4–binding complex by the TAP method, as described previously (16), and in Supplemental Figs. 1S-3S. We excised 30 well-separated bands that were specifically bound to IRF-4 from the gel, digested them with trypsin, and identified them by tandem mass spectrometry. However, only fourteen bands, in addition to IRF-4, were identified with significant scores ($p < 0.05$) in the Swiss-Prot database, using the MASCOT search engine (Supplemental Table S1). One of the peptide sequences acquired from the approximately 75–80 kDa protein band was matched to the human c-Rel proto-oncogene protein.

3.2. Specific binding between IRF-4 and c-Rel

We further analyzed the binding of c-Rel to IRF-4, because the enhanced expression of both c-Rel and IRF-4 is associated with the prognosis in ATLL patients (15,16). An HTLV-1 (human T-cell leukemia virus type 1)-infected T-cell line, HUT102, also expresses large amounts of IRF-4 and c-Rel. As shown in Fig. 1A, the IRF-4 antibody co-precipitated c-Rel with IRF-4 more effectively in the presence of 250ng/ml PMA and 1 μM Ionomycin (P/I), as compared to the control IgG. Conversely, the anti c-Rel antibody also co-precipitated IRF-4 with c-Rel independently of the P/I treatment, as compared to the control IgG (Fig. 1B). Since the amounts of IRF-4 and c-Rel were not affected by the P/I treatment, the enhanced binding by P/I indicated that the P/I treatment induced a functional change in IRF-4, c-Rel, or other binding molecules. In addition, we examined whether

IRF-4 directly binds to c-Rel, by over-expressing them in HEK293T cells. The HA-tagged IRF-4 was specifically co-precipitated with the FLAG-tagged c-Rel, and the binding was enhanced in the presence of P/I (Fig. 1C).

Next, we examined the region of c-Rel that is responsible for its interaction with IRF-4, using HA-tagged deletion mutants of c-Rel (Fig. 2A,B). The expected 68-kDa, 39-kDa, and 34-kDa bands for the full-length, N-terminal half (1-1174), and C-terminal half (1174-1860) c-Rel constructs, respectively, were detected with an anti-HA antibody (Fig. 2B, left). Each mutant c-Rel was co-expressed with FLAG-tagged IRF-4 in HEK293T cells and subjected to an immunoprecipitation assay. As shown in the right panel of Fig. 2B, the full-length and the N-terminal half (1-1174) c-Rel constructs interacted with IRF-4, in contrast to the C-terminal half (1174-1860). A strong band was detected always in the lanes containing FLAG-IRF-4. This may be related to IRF-4, however, the binding of the N-termial half c-Rel to IRF-4 was specific, because the C-terminal half c-Rel was not co-precipitated with FLAG-IRF-4 using the anti-FLAG antibody. On the other hand, the FLAG-tagged full-length and the C-terminal IRF association domain (403-1356) of the IRF-4 constructs co-precipitated HA-tagged c-Rel, in contrast to the N-terminal DNA-binding domain (1-405) of IRF-4 (Fig. 2C,D). These results indicated the interaction between the N-terminal half of c-Rel, containing the Rel homology domain, and the C-terminal IRF association domain of IRF-4.

3.3. IRF-4 and c-Rel cooperatively activate the IL-4 promoter

To explore the effects of c-Rel on the IRF-4 functions *in vivo*, we first examined the effects of c-Rel on the IRF-4-dependent IL-4 stimulation in HUT102 cells, using a luciferase reporter assay with an IL-4 promoter, because IRF-4 reportedly stimulated IL-4 expression

via a physical interaction with NFATc2 and/or NFATc1 (9,14). As shown in Fig. 3A, the P/I treatment enhanced the basal IL-4 promoter activities (the open vs. filled bars), and the IRF-4 (lane 4), c-Rel (lane 6), and IRF-4+c-Rel (lane 8) activities were significantly enhanced by 1.88±0.18-, 2.11±0.07-, and 4.47±0.55-fold, respectively, as compared to the basal IL-4 promoter (lane 2). Next, we tested the binding of IRF-4 and c-Rel to the IL-4 promoter region, using a ChIP assay. The amounts of the IRF-4 promoter region (-300 ~ -80) that co-precipitated with the anti-IRF-4, c-Rel, and control antibodies were determined semi-quantitatively, by changing the PCR cycle numbers (25, 30, and 35 cycles) in the presence or absence of P/I treatment (Fig. 3B). The specific binding of IRF-4 and c-Rel to the IL-4 promoter region was observed, and the binding was enhanced by the P/I treatment, as compared to the control lanes. The direct binding of IRF-4 and c-Rel each other, their binding to the IL-4 promoter, and the result that the increment of promoter activity by the both IRF-4 and c-Rel transfection (3.47-fold) was larger than the addition of each transfection (0.88- + 1.11- =1.99-fold), suggested that IRF-4 and c-Rel cooperatively activated the IL-4 promoter. However, we could not deny the possibility of that IRF-4 and c-Rel worked independently on the IL-4 promoter activation. The P/I treatment is often used to activate T cells, as well as the treatments with non-specific mitogens, specific T cell receptor (TCR) antigens, and the TCR antibodies. The optimal concentration and duration of the reagents were determined by measuring the amounts of mRNA with real-time PCR using specific primer sets for IL-2, and IL-4, as shown in Supplemental Fig.S4. When the EL-4 mouse T cells were treated with these reagents, Ionomycin only or PMA only was not enough to fully activate IL2 and IL4 promoters (Supplemental Figs. 4SA and 4SD). PMA activated the IL-2 and IL-4 promoters dose-dependently in the presence of 1μM Ionomycin,

and the mRNA expressions reached peak at 8h (Supplemental Figs. 4SB and 4SE). The plate-bound 0.5μg/ml anti-CD3, and 4μg/ml anti-CD28 also activated the IL-2 and IL-4 promoters (Supplemental Figs. 4SC and 4SF). We used 250ng/ml PMA, and 1μM Ionomycin, and plate-bound 0.5μg/ml anti-CD3, and 4μg/ml anti-CD28 for 4~8 hours to activate T cells otherwise indicated. The treatments with the same amounts of P/I were also employed to stimulate effectively $CD4^+$ T cells, and HUT102 cells.

3.4. IRF-4 and c-Rel activate the IL-2 promoter to produce IL-2

IRF-4 is reported to stimulate IL-2 production as well as IL-4 (14). To examine the effects of IRF-4 and c-Rel on the IL2-promoter, we introduced the plasmids encoding IRF-4 and c-Rel into HUT102 cells. We estimated the amount of IL-2 cDNA by applying different numbers of PCR cycles, after converting the mRNA to cDNA by reverse transcriptase, and evaluating the amount of β-actin cDNA as the total amount of mRNA. As shown in Fig. 4A, substantial amounts of IL-2 cDNA were detected in the presence of P/I, as compared to those in the absence of P/I, and the amount of IL-2 cDNA was increased by exogenously expressing c-Rel or IRF-4. To assess the data quantitatively, we employed the real-time PCR using IL-2 specific primers, and measured the mRNA expression of IL-2 relative to β-Actin (Fig.4B). In the presence of P/I, the exogenous IRF-4 and c-Rel appeared to increase the expression of IL-2 mRNA, but the enhancing effects were not significant ($p=0.116$ and 0.134). We think that the cooperation of IRF-4 with c-Rel was not observed, because HUT102 cells express a large amount of IRF-4, and thus the increases of IL-2 cDNA by IRF-4 or c-Rel were relatively small. Indeed, in EL-4 cells, a cooperative effect of IRF-4 with c-Rel on IL-2 production was observed, by measuring the amounts of IL-2 produced from the cells transfected with the plasmids encoding IRF-4 and c-Rel, using

an ELISA (Fig. 4C). However, any detectable amounts of IL-4 were not produced by any combinations of the reagents (Fig.4D). The roles of IRF-4 and c-Rel in IL-2 and IL-4 promoter activations are different in cell types and specific conditions. For example, c-Rel is indispensable for the optimal IL-2 production in naïve T-cells, but is not required in for the IL-2 production in blast T-cells (19). IRF-4 is also reported to differentially regulates the production of Th2 cytokines including IL-4 in naïve vs. effector/memory $CD4^+$ T cells (20). The specific roles of the c-Rel and IRF-4 interaction in the activation of the IL-2 and IL-4 promoters should be elucidated in specific cells and proper conditions.

3.5. Optimal IL-2 amd IL-4 productions require IRF-4 in vivo

Next, we examined the effects of IRF-4 on IL-2 and IL-4 productions *in vivo* using IRF-$4^{-/-}$ mice, because the IRF-4 and c-Rel interaction reminded us of the similar T-cell phenotypes between IRF-$4^{-/-}$ mice and c-$Rel^{-/-}$ mice (both mice exhibited defects in T-cell proliferation and IL-2 production in response to anti-CD3 stimulation). In addition, Banerjee et al. reported that cytokine-mediated priming of naïve T-cells was c-Rel-dependent (19). Therefore, we measured the IL-2 and IL-4 expressions in splenic $CD4^+$ T-cells from normal and IRF-$4^{-/-}$ mice, by anti-CD3 stimulation with and without TNF-α pretreatment. The amount of IL-2 mRNA in IRF-4-deficient cells (IRF-$4^{-/-}$) was significantly lower than that in normal cells, as evaluated by quantitative real time PCR (WT) (Fig. 5A). These results indicated that not only c-Rel but also IRF-4 is required for the optimal production of IL-2 in TNF-α-primed T-cells. On the other hand, we could not detect any IL-4 mRNA by anti-CD3 stimulation even in TNF-α-primed T-cells from WT or IRF-$4^{-/-}$ mice (Fig. 5B).

We further examined the effects of complete Freund's adjuvant (CFA)-mediated priming on the IL-2 production in splenic $CD4^+$ T-cells. Naive T-cells from CFA-primed

normal (WT), but not IRF-4$^{-/-}$, mice produced high levels of IL-2 in response to anti-CD3 stimulation (termed superinduction), dependent on the amount of TCRβ antibody (Fig. 5C). The priming effect of CFA was completely absent in the IRF-4-deficient T-cells. To elucidate the mechanism of high IL-2 production, we examined the priming effects on the IL-2 promoter activity by measuring IL-2 mRNA with real time PCR (Fig.6A). The IL-2 mRNA amounts enhanced by TCR stimulation with the anti-CD3 and anti-CD28 antibodies were CFA-dependent in the WT mice-derived CD4^{+} T-cells. The CFA-dependent superinduction was disappeared in IRF-4$^{-/-}$ mice, as reported in c-Rel$^{-/-}$ mice. These indicated that IRF-4 as well as c-Rel is indispensable to fully activate IL-2 promoter *in vivo*.

As for IL-4 regulation, the IL-4 production stimulated with TCRβ antibody was also dependent on the CFA priming in WT, although the amounts of IL-4 were much smaller than those of IL-2 (Figs. 5C and 5D). The TCR activation-dependent IL-4 mRNA amounts were significantly lower in the IRF-4$^{-/-}$ mice compared to WT mice, but the CFA-dependence was not observed (Fig. 6B) These suggested that the regulations of IRF-4 may be different in the IL-2 and IL-4 promoters. The discrepancy between the protein and mRNA levels of IL-4 may be caused by the effects of IRF-4 on the stability of IL-4 protein, in addition to the effects on the promoter. Another possibility of the discrepancy between the IL-4 protein and mRNA levels was due to the different sensitivities of the detection systems employed here. The differences in mRNA expression measured at 4h after TCR stimulation may be not enough to assess the IL-4 promoter activities, considering that the IL-4 protein levels measured by ELISA reflect the continuous effects during 16 hours, and that the differences of IL-4 amounts were much smaller than those of IL-2.

4. Discussion

In the present study, we isolated a protein complex associated with IRF-4 in HTLV-1-infected T-cells using the TAP method, and showed that an NF-κB family member, c-Rel, physically associates with IRF-4 and enhances the IRF-4-dependent IL-4 and IL-2 promoter activation in some T-cells. In addition, we mapped their binding sites to the C-terminal IRF association domain of IRF-4, and the N-terminal Rel-homology domain of c-Rel (Fig. 2). Considering that these domains are used for interactions with other IRF members and NF-kB members, respectively, their interactions may affect the various functions of important transcription factors involved in cell growth, cell death, immunity, and other phenomena (1,21). Although FKBP52, PU.1, E47, BCL6, STAT6, NFATc2, NFATc1, IBP, and MyD88 have been reported to bind to IRF-4 so far (9,13,21,22,23), the interaction of IRF-4 with c-Rel and their functional cooperation to enhance the IL-2 and IL-4 promoter activities (Figs. 3 and 4) are noteworthy. IRF-4 was indispensable for the optimal IL-2 and IL-4 productions *in vivo* was evident (Figs. 5 and 6), although the precise mechanism of the cooperation between IRF-4 and c-Rel in the regulation of the cytokine productions should be elucidated. First, the elevated expression of IRF-4 and c-Rel is closely correlated with the exacerbation of ATLL (24) and antiviral therapy resistance in ATLL (15). The antiviral therapy consists of azidothymidine (AZT) and IFNα, which work at various points to prevent virus infection and proliferation. Considering the fact that the IFNα pathway can cross-talk with the IFNγ pathway (25), one possible mechanism related to the antiviral resistance is that IRF-4 antagonizes the INFγ-mediated IRF1-dependent suppression of the IL-4 promoter (26), by interacting with each other through the IRF association domains, or competing with each other for binding to the same

DNA sites (IFN-stimulated response elements (ISREs) are located at the proximal region of IL-4 promoter) (Fig. 3B) or a common adaptor, MyD88 (23). On the other hand, c-Rel and IRF-4 themselves reportedly activate the IRF-4 promoter (8,27). The enhancing loop and their cooperation may effectively activate the downstream genes, including the strong T-cell growth factor IL-2 (Fig. 4) and the proto-oncogene c-myc (8). The determination of the interacting sites between IRF-4 and c-Rel will give precious information to develop specific reagents inhibiting T-cell growth in ATLL patients.

Second, the IRF-4-dependent IL-4 induction in the presence of P/I was reportedly enhanced by the calcineurin-regulated transcription factors NFATc2 (NFAT1) and/or NFATc1 (NFAT2), and may partly explain the crucial roles of IRF-4 in Th2 differentiation (9,12,25). However, we could not detect any specific binding of endogenous IRF-4 or c-Rel with NFATc1 or NFATc2 in the presence or absence of P/I treatment in HUT102 or EL-4 T-cells, although the exogenously-expressed NFATc1 and NFATc2 showed very weak binding to IRF-4 even in the presence of P/I in 293T cells (data not shown). Considering the redundant and complicated effects of NFAT protein families (NFATc1, NFATc2, and NFAT4 are expressed in T-cells) (28) on the IL-4 promoter activity, and that the substantial interaction of IRF-4 with c-Rel to activate the IL-4 promoter did not require P/I treatment (Figs. 1~3), we think the P/I-dependent enhancement is not simply because of the binding of IRF-4 with the NFATs. IRF-4 was indispensable for the optimal IL-4 production, but the mechanism was not explained only by the effects on the IL-4 promoter activation (Figs. 4~6).

In contrast, our data suggested that IRF-4 worked mainly on the IL-2 promoter activation, and the activation was may be in cooperation with c-Rel. The IL-2 promoter

activation by IRF-4 required P/I treatment or TCR stimulation with cytokine priming (Fig. 4~6). These results suggested that qualitative changes of IRF-4 and/or c-Rel, their possible interacting molecules, and the chromatin structure in the IL-2 proximal promoter region by such as phosphorylation, acetylation, and demethylation may be necessary for optimal IL-2 promoter activation (29). The absence of ISRE site in the IL-2 proximal promoter region, compared to the IL-4 promoter, may be involved in the difference. In addition, c-Rel was recently reported to be required for the development of thymic $Foxp3^{+}$ CD4 regulatory T-cells (Treg) (30), and Foxp3-dependent IRF-4 induction in Treg is thought to be important for the Treg function to control the Th2 response (31). Therefore, regulating the interaction between IRF-4 and c-Rel by manipulating the molecules may help to differentiate from pluripotent T-cells into specific lineage to treat various diseases (32).

In conclusion, the elucidation of the physical and functional cooperation between IRF-4 and c-Rel to activate of the IL-4 and IL-2 genes in T-cells, is important for future gene therapy for ATLL by abolishing their growth effects, and to present promising targets for adoptive immunotherapy by regulating specific T-cell development.

Acknowledgements

We thank R. Moriuchi, and H. Udono and T. Mori (Nagasaki University Graduate School of Biomedical Sciences) for the TAP tag expression plasmid, and for LC/MS/MS technical assistance, respectively; S. Yamaoka (Tokyo Medical Dental University School of Medicine) for the human c-Rel expressing plasmid and the 293T cell line; and T. W. Mak (Ontario Cancer Institute, Amgen Institute) for the anti-IRF-4 rabbit polyclonal antibody. This work was supported by Grants-in-Aid from the Ministry of Education, Culture, Sports, Science and Technology of Japan, and by the Global Center of Excellence Program at Nagasaki University.

References

[1] D. Savitsky, T. Tamura, H. Yanai, T. Taniguchi, Regulation of immunity and oncogenesis by the IRF transcription factor family, Cancer Immunol. Immunother. 59 (2010) 489-510.

[2] T. Matsuyama, A. Grossman, H.W. Mittrucker, et al., Molecular cloning of LSIRF, a lymphoid-specific member of the interferon regulatory factor family that binds the interferon-stimulated response element (ISRE), Nucleic Acids Res. 23 (1995) 2127-2136.

[3] C.F. Eisenbeis, H. Singh, U. Storb, Pip, a novel IRF family member, is a lymphoid-specific, PU.1-dependent transcriptional activator, Genes Dev. 9 (1995) 1377-1387.

[4] T. Yamagata, J. Nishida, S. Tanaka, et al., A novel interferon regulatory factor family transcription factor, ICSAT/Pip/LSIRF, that negatively regulates the activity of interferon-regulated genes, Mol. Cell. Biol. 16 (1996) 1283-1294.

[5] H.W. Mittrucker, T. Matsuyama, A. Grossman, et al., Requirement for the transcription factor LSIRF/IRF4 for mature B and T lymphocyte function, Science 275 (1997) 540-543.

[6] A.L. Brass, A.Q. Zhu, H. Singh, Assembly requirements of PU.1-Pip (IRF-4) activator complexes: inhibiting function in vivo using fused dimmers, EMBO J. 18 (1999) 977-991.

[7] A.L. Shaffer, N.C. Emre, P. B. Romesser, L.M. Staudt, IRF4: Immunity. Malignancy! Therapy?, Clin. Cancer Res. 15 (2009) 2954-2961.

[8] A.L. Shaffer, N.C. Emre, L. Lamy, et al., IRF4 addiction in multiple myeloma, Nature 454 (2008) 226-231.

[9] J. Rengarajan, K. Mowen, K. McBride, E. Smith, H. Singh, L. Glimcher, Interferon regulatory factor 4 (IRF4) interacts with NFATc2 to modulate interleukin 4 gene expression,

J. Exp. Med. 195 (2002) 1003-1012.

[10] N. Tominaga, K. Ohkusu-Tsukada, H. Udono, R. Abe, T. Matsuyama, K. Yui, Development of Th1 and not Th2 immune responses in mice lacking IFN-regulatory factor-4, Int. Immunol. 15 (2003) 1-10.

[11] S. Suzuki, K. Honma, T. Matsuyama, et al., Critical roles of interferon regulatory factor 4 in CD11bhighCD8alpha-dendritic cell development, Proc. Natl. Acad. Sci. USA 101 (2004) 8981-8986.

[12] J. Gilmour, P. Lavender, Control of IL-4 expression in T helper 1 and 2 cells, Immunology 124 (2008) 437-444.

[13] Y. Mamane, S. Sharma, L. Petropoulos, R. Lin, J. Hiscott, Posttranslational regulation of IRF-4 activity by the immunophilin FKBP52, Immunity 12 (2000) 129-140.

[14] C.M. Hu, S.Y. Jang, J.C. Fanzo, A.B. Pernis, Modulation of T cell cytokine production by interferon regulatory factor-4, J. Biol. Chem., 277 (2002) 49238-49246.

[15] J. C. Ramos, P. Ruiz Jr., L. Ratner, et al., IRF-4 and c-Rel expression in antiviral resistant adult T-cell leukemia/lymphoma, Blood 109 (2007) 3060-3068.

[16] O. Puig, F. Caspary, G. Rigaut, et al., The tandem affinity purification (TAP) method: a general procedure of protein complex purification, Methods 24 (2001) 218-229.

[17] E. Brownell, N. Mittereder, N.R. Rice, A human rel proto-oncogene cDNA containing an Alu fragment as a potential coding exon, Oncogene 4 (1989) 935-942.

[18] M.M. Müller, E. Schreiber, W. Schaffner, P. Matthias, Rapid test for in vivo stability and DNA binding of mutated octamer binding proteins with 'mini-extracts' prepared from transfected cells, Nucleic Acids Res. 17 (1989) 6420.

[19] D. Banerjee, H.C. Liou, R. Sen, c-Rel-dependent priming of naive T cells by inflammatory cytokines. Immunity 23 (2005) 445-458.

[20] Honma K, Kimura D, Tominaga N, Miyakoda M, Matsuyama T, Yui K. Interferon regulatory factor 4 differentially regulates the production of Th2 cytokines in naive vs. effector/memory CD4+ T cells. Proc Natl Acad Sci U S A. 105 (2008) 15890-15895.

[21] K. Honda, T. Taniguchi, IRFs: master regulators of signalling by Toll-like receptors and cytosolic pattern-recognition receptors, Nat. Rev. Immunology 6 (2006) 644-658.

[22] Q. Chen, W. Yang, S. Gupta, et al., IRF-4-binding protein inhibits interleukin-17 and interleukin-21 production by controlling the activity of IRF-4 transcription factor, Immunity 29 (2008) 899-911.

[23] H. Negishi, Y. Ohba, H. Yanai, et al., Negative regulation of Toll-like-receptor signaling by IRF-4, Proc. Natl. Acad. Sci. USA 102 (2005) 15989-15994.

[24] Y. Imaizumi, T. Kohno, Y. Yamada, et al., Possible involvement of interferon regulatory factor 4 (IRF4) in a clinical subtype of adult T-cell leukemia, Jpn. J. Cancer Res. 92 (2001) 1284-1292.

[25] K. Schroder, P.J. Hertzog, T. Ravasi, D.A. Hume, Interferon-gamma: an overview of signals, mechanisms and functions, J. Leukoc. Biol. 75 (2004) 163-189.

[26] M. Li-Weber, P.H. Krammer, Regulation of IL4 gene expression by T cells and therapeutic perspectives, Nat. Rev. Immunol. 3 (2003) 534-543.

[27] R. J. Grumont, S. Gerondakis, Rel induces interferon regulatory factor 4 (IRF-4) expression in lymphocytes: modulation of interferon-regulated gene expression by rel/nuclear factor kappaB, J. Exp. Med. 191 (2000) 1281-1292.

[28] F. Macian, NFAT proteins: key regulators of T-cell development and function, Nat. Rev. Immunol. 5 (2005) 472-484.

[29] H.P. Kim, J. Imbert, W.J. Leonard, Both integrated and differential regulation of components of the IL-2/IL-2 receptor system, Cytokine Growth Factor Rev. 17 (2006) 349-366.

[30] I. Isomura, S. Palmer, R.J. Grumont, et al., c-Rel is required for the development of thymic Foxp3+ CD4 regulatory T cells, J. Exp. Med. 206 (2009) 3001-3014.

[31] Y. Zheng, A. Chaudhry, A. Kas, et al., Regulatory T-cell suppressor program co-opts transcription factor IRF4 to control T(H)2 responses, Nature 458 (2009) 351-356.

[32] P.S. Kim, R. Ahmed, Features of responding T cells in cancer and chronic infection, Curr. Opin. Immunol. 22 (2010) 223-230.

Figure legends

Fig. 1 IRF-4 and c-Rel binding. (**A, B**) Nuclear extracts from HUT102 cells ($5x10^6$), cultured for 8h in the presence or absence of 250ng/ml PMA and 1 μM Ionomycin (P/I), were immunoprecipitated with the IRF-4 antibody (**A**) or the c-Rel antibody (**B**). The SDS-PAGE fractionated proteins were blotted with the c-Rel antibody (**A**) and the IRF-4 antibody (**B**), respectively. (**C**) HEK293T cells ($4x10^5$) were transfected with an HA-tagged IRF-4 expression plasmid and/or Flag-tagged c-Rel expression plasmid (500ng each), using the FuGENE reagent. Two days after transfection, the cells were incubated for 8h in the presence or absence of P/I. The nuclear extracts were prepared, immunoprecipitated with an anti-FLAG antibody, and blotted with an anti-HA antibody.

Fig. 2 Determination of IRF-4 and c-Rel binding sites. (**A, B**) HA-tagged full-length, N-terminal half (1-1174), and C-terminal half (1174-1860) c-Rel constructs (500ng each) were introduced with FLAG-tagged full-length IRF-4 (500ng) into $4x10^5$ HEK293T cells in 6-well plates. The lysates (**B,** left panel), and the c-Rel deletion mutants co-immunoprecipitated with IRF-4 by the anti-FLAG antibody (**B**, right panel) were detected with an anti-HA antibody. The arrows indicate the HA-c-Rel bands, and the arrowhead shows a non-specific band. (**C, D**) FLAG-tagged full-length, N-terminal region (1-405), and C-terminal region (403-1356) IRF-4 constructs (500ng each) were introduced with HA-tagged full-length c-Rel (500ng) into $4x10^5$ HEK293T cells in 6-well plates. The lysates (**D,** left panel), and the c-Rel co-immunoprecipitated with the IRF-4 deletion mutants by the anti-FLAG antibody (**D**, right panel), were probed with an anti-HA antibody. The arrows and arrowhead indicate the FLAG-IRF-4 bands, and the HA-c-Rel band, respectively.

Fig. 3 IRF-4 and c-Rel co-operatively activate the human IL-4 promoter. (**A**) HUT102 cells ($2x10^5$) were transfected with a luciferase reporter construct driven by the human IL-4 promoter (-250 ~ +15) (1μg) with/without IRF-4, and c-Rel expression plasmids (200 ng each) by electroporation. Two days after transfection, the cells were incubated for 8hr in the presence or absence of 250ng/ml PMA and 1 μM Ionomycin (P/I), and the luciferase activities were measured. Results show the mean ± S.E. of three independent experiments. (**B**) The chromatin immunoprecipitation (ChIP) assay was performed using HUT102 cells ($5x10^6$) treated with/without P/I for 8h, with anti-IRF-4 and anti-c-Rel antibodies. The amount of specifically precipitated DNA was determined semi-quantitively, by changing the PCR cycle numbers (25, 30 and 35 cycles) with primers specific for the IL4 promoter (-300～-80).

Fig. 4 IRF-4 and c-Rel activate the IL-2 promoter to produce IL-2.

HUT102 cells ($4x10^5$) were transfected with IRF-4 and c-Rel expression plasmids (2μg each) by electroporation. Two days after transfection, the cells were incubated for 8hr in the presence or absence of 250ng/ml PMA and 1 μM Ionomycin (P/I), and the total RNA was extracted. The amounts of IL-2 and β-actin cDNAs were estimated by applying different numbers of PCR cycles (**A**), and measured by real time PCR using the specific primers (**B**). The EL-4 cells ($2x10^5$) were transfected with IRF-4 and c-Rel expression plasmids (500 ng each) by electroporation. Two days after transfection, the cells were incubated for 8hr in the presence or absence of P/I, and the amounts of IL-2 (**C**), and IL-4 (**D**) in the supernatant were measured by sandwich ELISA. The data shown are representative of three independent experiments done in triplicate.

Fig. 5 IRF-4 is indispensable to produce IL-2 and IL-4 production *in vivo*.

(**A, B**) TNF-α-mediated priming of naive T-cells requires IRF-4. $CD4^+$ T-cells were purified from the spleens of C57BL/6 mice (WT) or IRF-$4^{-/-}$ mice, and were activated with 5 ng/ml of TNF-α or with TNF-α plus anti-CD3 antibody (10 μg/ml) for 6h. The relative amounts of IL-2 (**A**) and IL-4 (**B**) mRNA normalized to the quantity of G3PDH mRNA were determined by real-time PCR, using the reverse-transcribed cDNAs. The data shown are representative of three independent experiments done in triplicate. (**C, D**) Adjuvant-mediated priming of naive T-cells also requires IRF-4. C57BL/6 mice (WT) and IRF-$4^{-/-}$ mice were injected intraperitoneally with complete Freund's adjuvant (CFA) or saline (PBS), followed by a second injection of incomplete Freund's (IFA) or PBS, respectively. Six days later, splenic T-cells were activated with various amounts of plate-bound anti-TCRβ antibody, and the levels of IL-2 (**C**), and IL-4 (**D**) were determined by an ELISA. Data shown are representative of three independent experiments.

Fig. 6 Effects of IRF-4 on the IL-2 and IL-4 promoters *in vivo*.

C57BL/6 mice (WT) and IRF-$4^{-/-}$ mice were injected intraperitoneally with complete Freund's adjuvant (CFA) or saline (PBS), followed by a second injection of incomplete Freund's (IFA) or PBS, respectively. Six days later, splenic T-cells were activated with various amounts of plate-bound anti-CD3, and anti-CD28 antibodies, and the relative amounts of IL-2 mRNA (**C**), and IL-4 mRNA (**D**) normalized to the quantity of β-Actin mRNA were determined by real time PCR. Data shown are representative of three independent experiments.

Fig.1

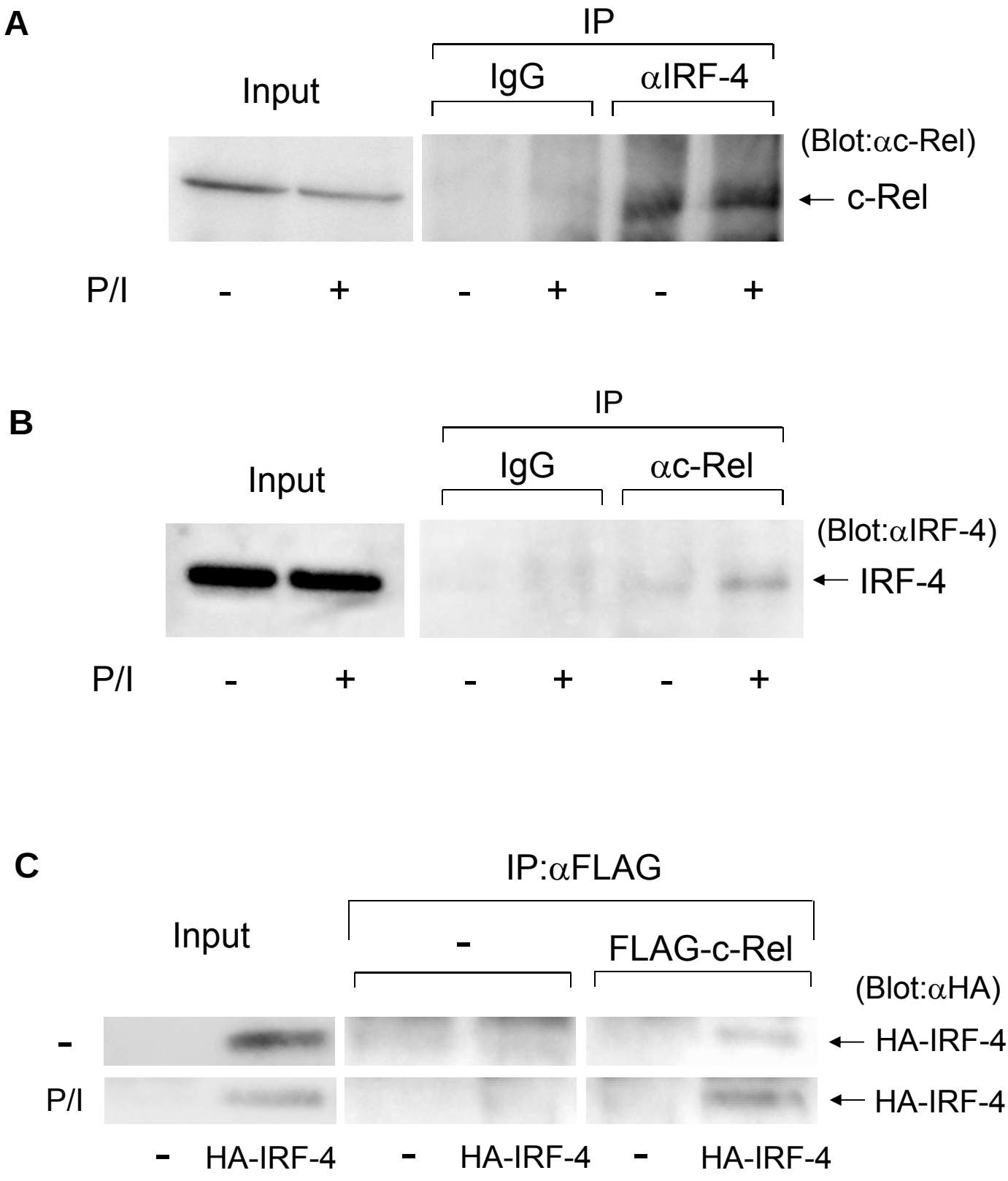
A
IP
Input
IgG
αIRF-4
(Blot:αc-Rel)
← c-Rel
P/I - + - + - +
B
IP
Input
IgG
αc-Rel
(Blot:αIRF-4)
← IRF-4
P/I - + - + - +
C
IP:αFLAG
Input
-
FLAG-c-Rel
(Blot:αHA)
-
← HA-IRF-4
P/I
← HA-IRF-4
- HA-IRF-4 - HA-IRF-4 - HA-IRF-4

Fig.2

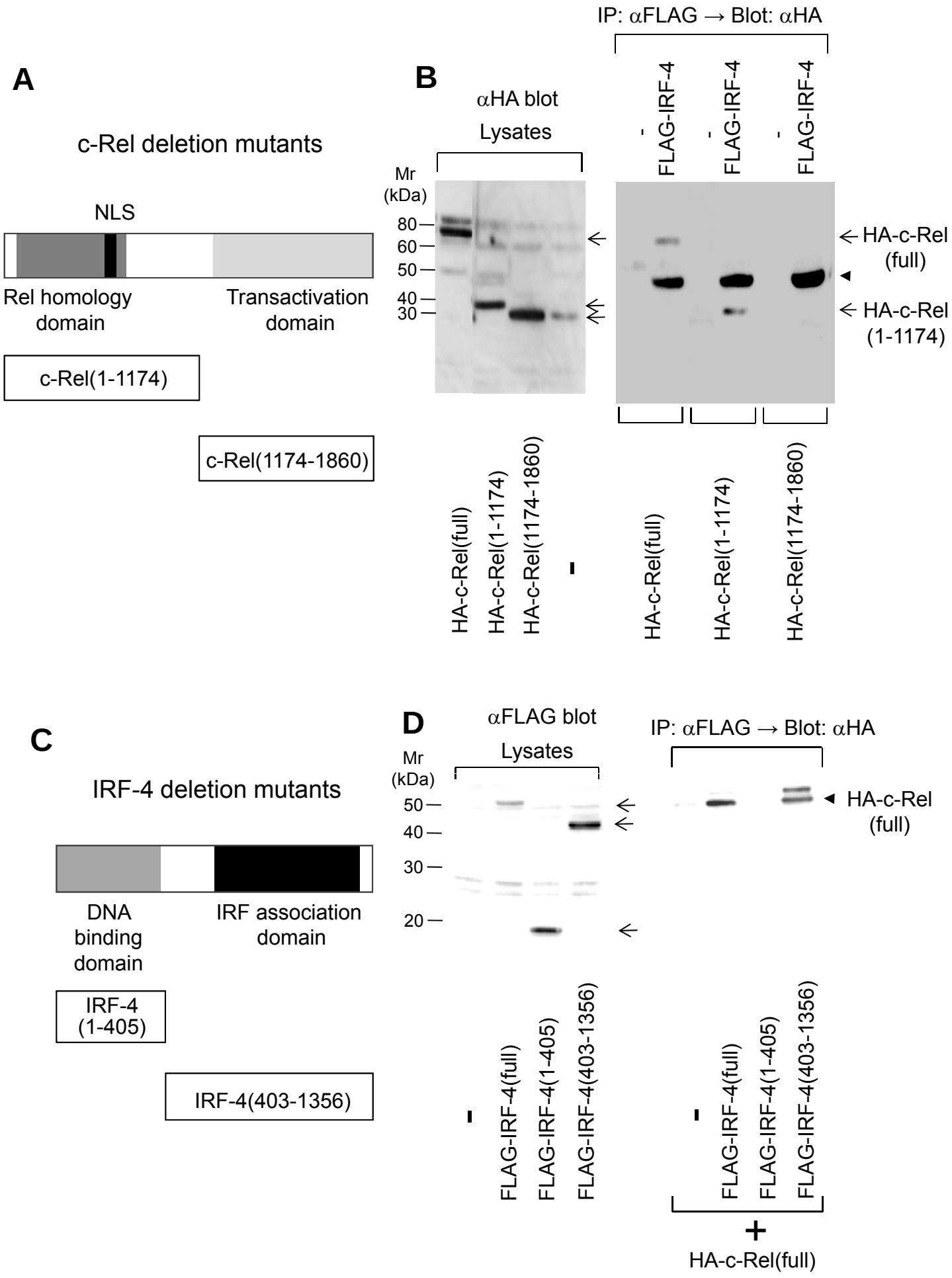
A
c-Rel deletion mutants
NLS
Rel homology domain
Transactivation domain
c-Rel(1-1174)
c-Rel(1174-1860)
B
αHA blot
Lysates
Mr (kDa)
80
60
50
40
30
IP: αFLAG → Blot: αHA
- FLAG-IRF-4
- FLAG-IRF-4
- FLAG-IRF-4
HA-c-Rel (full)
HA-c-Rel (1-1174)
HA-c-Rel(full)
HA-c-Rel(1-1174)
HA-c-Rel(1174-1860)
-
HA-c-Rel(full)
HA-c-Rel(1-1174)
HA-c-Rel(1174-1860)
C
IRF-4 deletion mutants
DNA binding domain
IRF association domain
IRF-4 (1-405)
IRF-4(403-1356)
D
αFLAG blot
Lysates
Mr (kDa)
50
40
30
20
IP: αFLAG → Blot: αHA
HA-c-Rel (full)
-
FLAG-IRF-4(full)
FLAG-IRF-4(1-405)
FLAG-IRF-4(403-1356)
-
FLAG-IRF-4(full)
FLAG-IRF-4(1-405)
FLAG-IRF-4(403-1356)
+
HA-c-Rel(full)

Fig.3

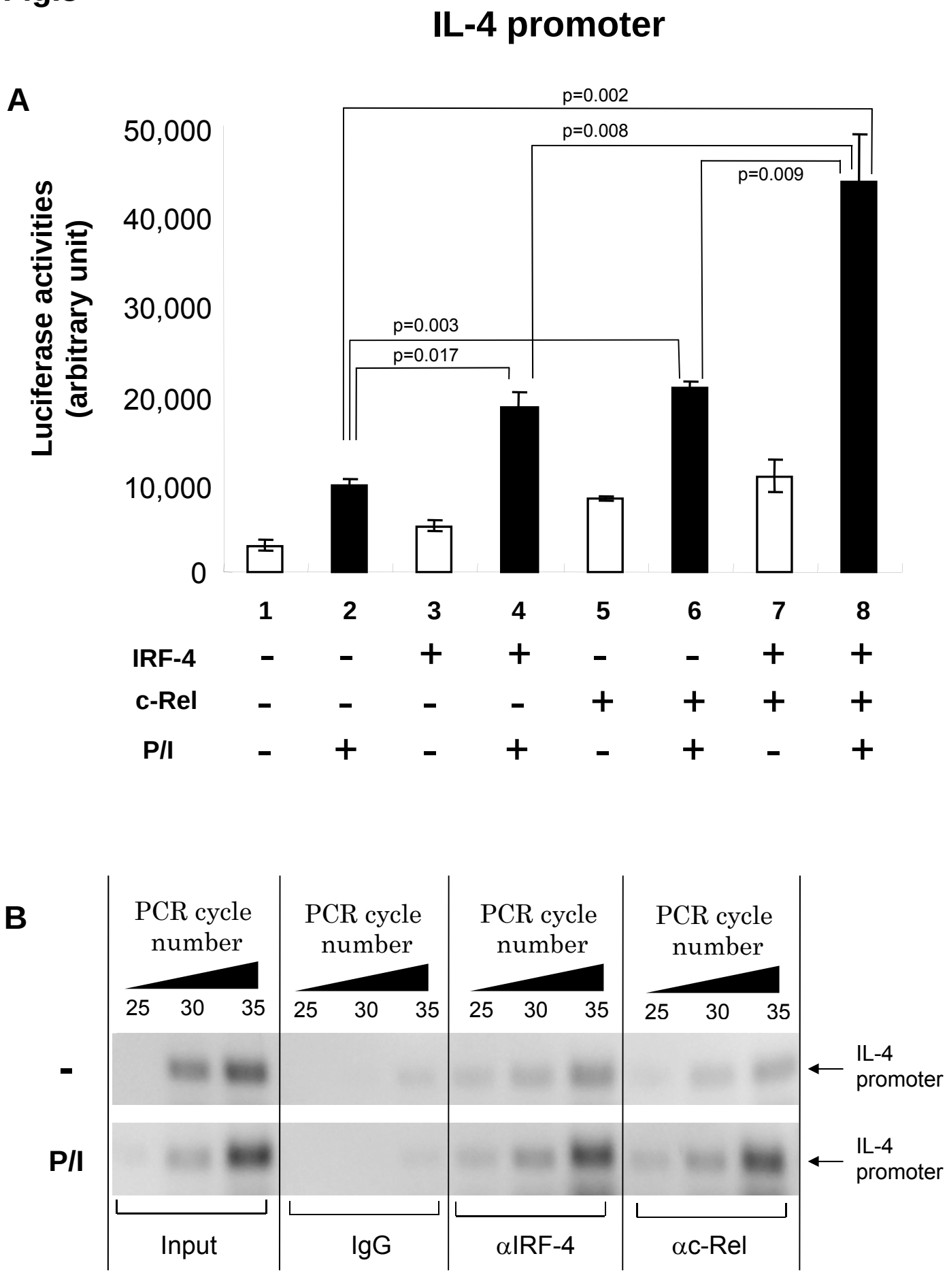
IL-4 promoter
A
Luciferase activities (arbitrary unit)
50,000
40,000
30,000
20,000
10,000
0
p=0.002
p=0.008
p=0.009
p=0.003
p=0.017
1 2 3 4 5 6 7 8
IRF-4 - - + + - - + +
c-Rel - - - - + + + +
P/I - + - + - + - +
B
PCR cycle number
25 30 35
-
P/I
IL-4 promoter
Input
IgG
αIRF-4
αc-Rel

Fig.4

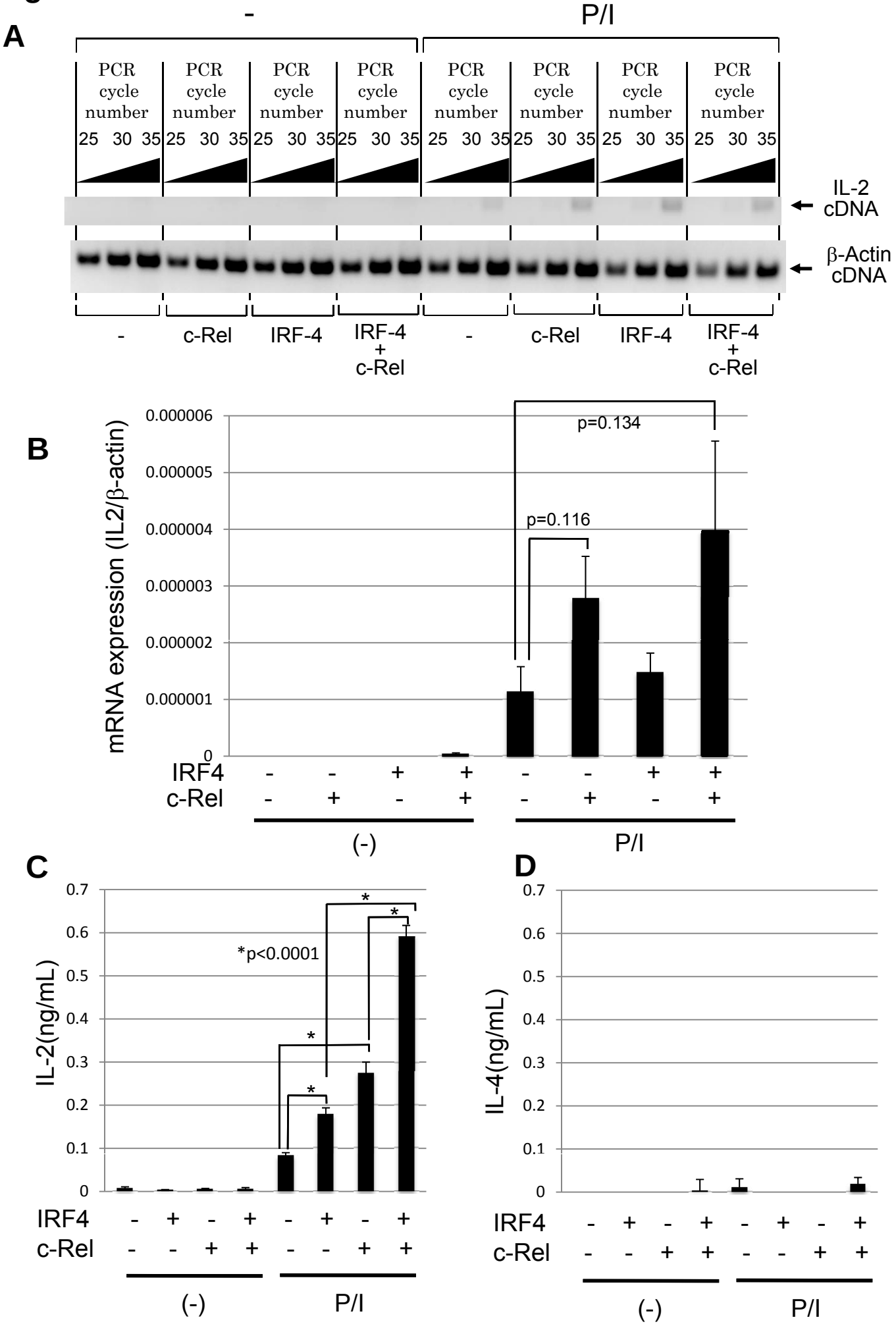
A
-
P/I
PCR cycle number
25 30 35
IL-2 cDNA
β-Actin cDNA
-
c-Rel
IRF-4
IRF-4 + c-Rel
B
mRNA expression (IL2/β-actin)
0.000006
0.000005
0.000004
0.000003
0.000002
0.000001
0
p=0.134
p=0.116
IRF4
c-Rel
(-)
P/I
C
IL-2(ng/mL)
0.7
0.6
0.5
0.4
0.3
0.2
0.1
0
*p<0.0001
*
IRF4
c-Rel
(-)
P/I
D
IL-4(ng/mL)
0.7
0.6
0.5
0.4
0.3
0.2
0.1
0
IRF4
c-Rel
(-)
P/I

Fig.5

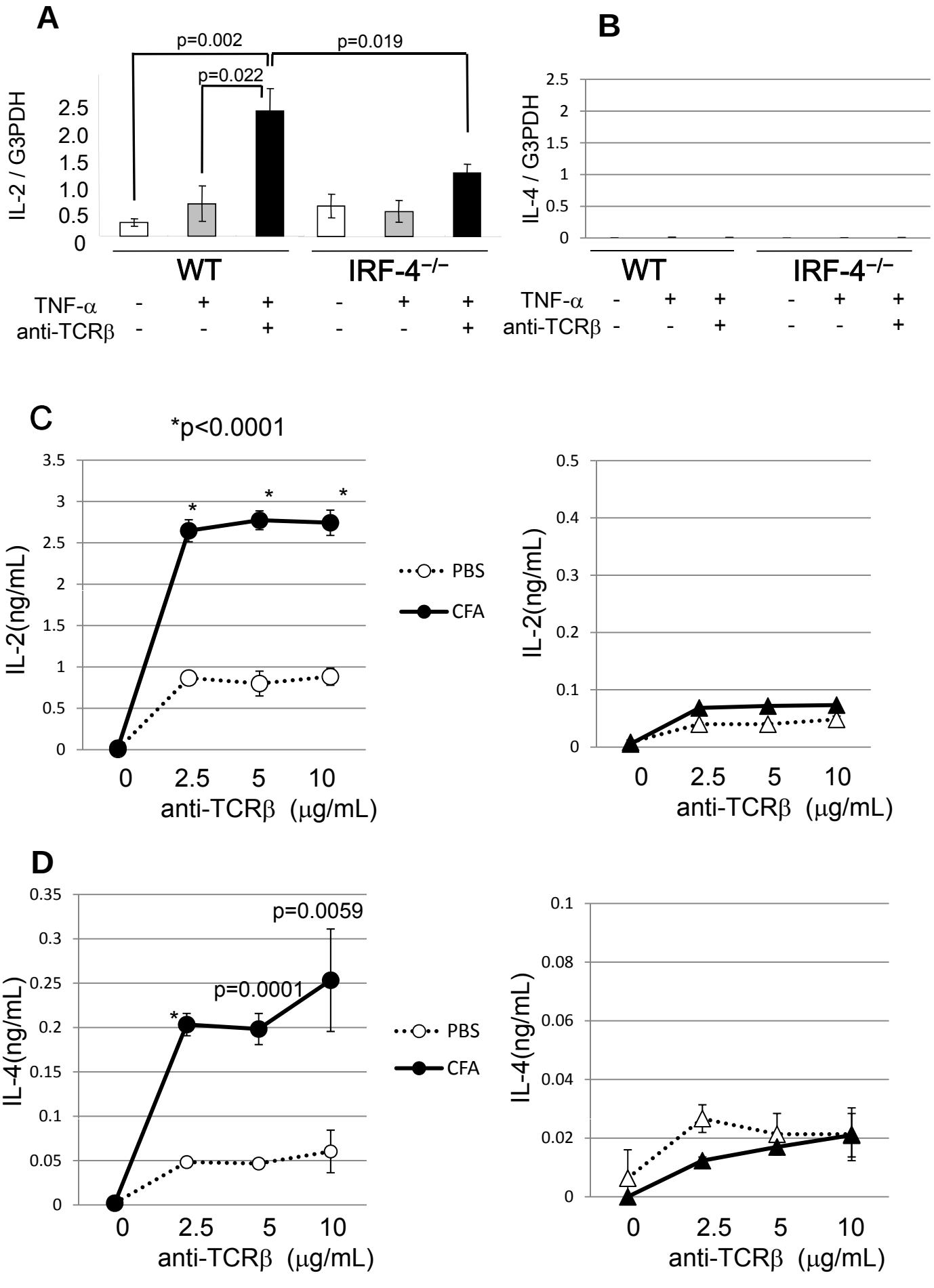
A
p=0.002
p=0.019
p=0.022
IL-2 / G3PDH
2.5
2.0
1.5
1.0
0.5
0
WT
IRF-4−/−
TNF-α - + + - + +
anti-TCRβ - - + - - +
B
IL-4 / G3PDH
2.5
2
1.5
1
0.5
0
WT
IRF-4−/−
TNF-α - + + - + +
anti-TCRβ - - + - - +
C
*p<0.0001
IL-2(ng/mL)
3.5
3
2.5
2
1.5
1
0.5
0
0 2.5 5 10
anti-TCRβ (μg/mL)
PBS
CFA
IL-2(ng/mL)
0.5
0.4
0.3
0.2
0.1
0
0 2.5 5 10
anti-TCRβ (μg/mL)
D
IL-4(ng/mL)
0.35
0.3
0.25
0.2
0.15
0.1
0.05
0
p=0.0059
p=0.0001
0 2.5 5 10
anti-TCRβ (μg/mL)
PBS
CFA
IL-4(ng/mL)
0.1
0.08
0.06
0.04
0.02
0
0 2.5 5 10
anti-TCRβ (μg/mL)

Fig.6

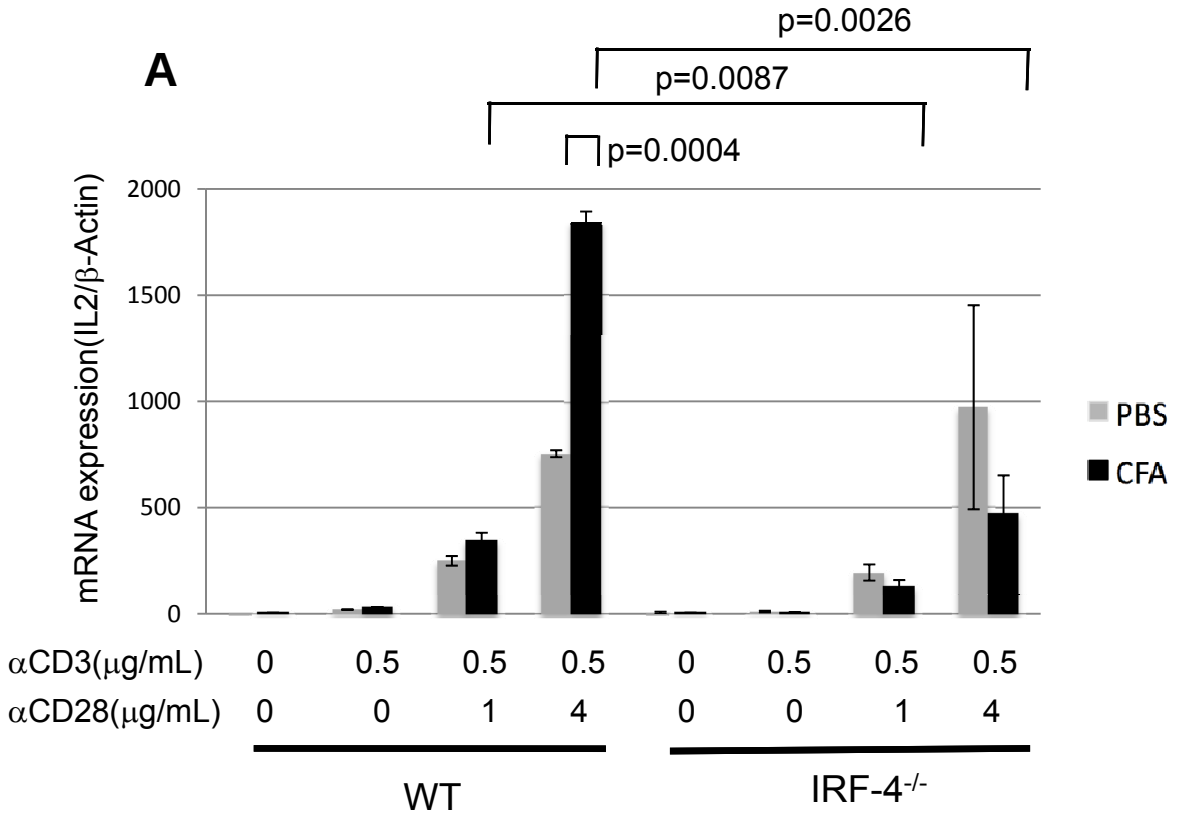
A
p=0.0026
p=0.0087
p=0.0004
mRNA expression(IL2/β-Actin)
2000
1500
1000
500
0
PBS
CFA
αCD3(μg/mL) 0 0.5 0.5 0.5 0 0.5 0.5 0.5
αCD28(μg/mL) 0 0 1 4 0 0 1 4
WT
IRF-4-/-

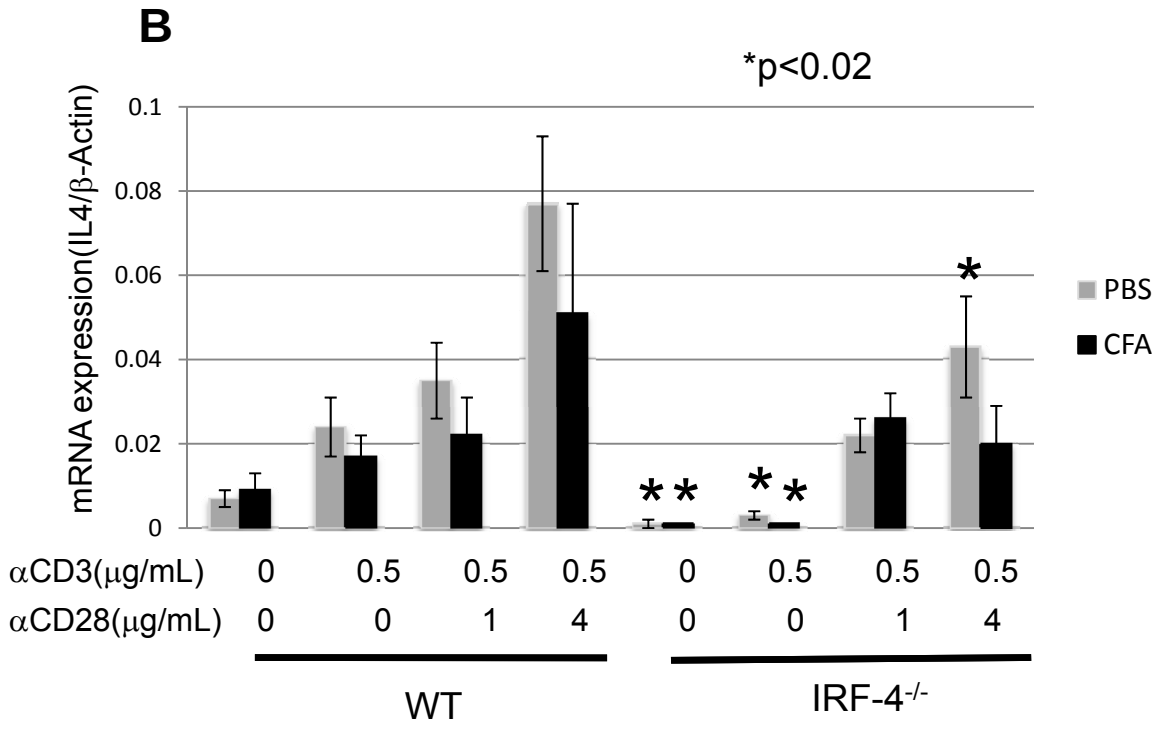
B
*p<0.02
mRNA expression(IL4/β-Actin)
0.1
0.08
0.06
0.04
0.02
0
PBS
CFA
αCD3(μg/mL) 0 0.5 0.5 0.5 0 0.5 0.5 0.5
αCD28(μg/mL) 0 0 1 4 0 0 1 4
WT
IRF-4-/-

Supplemental material

Materials and Methods

Plasmid constructs and transfection

For the TAP purification, HUT102 cells were transfected with the TAP-IRF4 plasmid using the TransFast Transfection Reagent (Promega). The TAP tag cassette consists of, N to C termini, Calmodulin-binding peptide (CBP), the tobacco etch virus, TEV protease recognition sequence (TEV site), and two copies of IgG binding domain of Staphylococcus aureus Protein A (IGB). A full-length human IRF-4 cDNA lacking the TGA stop codon was inserted before the TAP tag cassette site of the pcDNA3.1-derived plasmid.

Preparation of cell extracts

HUT102 cells (1×10^8 cells) transfected with or without the TAP-tagged IRF-4, were collected, suspended in 2ml of buffer A (10mM HEPES, pH7.9, 10mM KCl, 0.1mM EDTA, 1mM DTT, and 0.5mM PMSF), and then lysed in the presence of 0.6% Nonidet P-40 by vortex. The nuclei were collected by brief centrifugation, and were resuspended in 800 μl of buffer C (20mM HEPES, pH7.9, 400mM NaCl, 1mM EDTA, 1mM DTT and 1mM PMSF). The nuclear proteins were extracted by incubating for 15min at 4°C, and cleared by centrifugation at 15,000 rpm for 5 min at 4°C.

Tandem affinity purification (TAP)

The purification was performed by incubating 800μl of the nuclear extract with 100μl of IgG Sepharose beads (Amersham Biosciences) in 5ml of IPP150 buffer (10mM Tris-HCl, pH8.0, 150mM NaCl, and 0.1%NP-40) for 2h at 4°C. The mixture was poured into an Econocolumn (Bio-Rad), and the beads were washed extensively with IPP150 buffer

and once with TEV cleavage buffer (10mM Tris-HCl, pH8.0, 15mM NaCl, 0.1%NP-40, 0.5mM EDTA, and 1mM DTT). The beads were suspended in 1ml of TEV cleavage buffer and were incubated with 100 units of TEV protease (Invitrogen) by rotation for 2h at 16°C. The eluate was recovered by centrifugation, and then incubated with the 100μl of calmodulin beads in 3ml of calmodulin binding buffer (10mM Tris-HCl, pH8.0, 150mM NaCl, 0.1%NP-40, 10mM 2-mercaptoethanol, 1mM magnesium acetate, 1mM imidazole, and 2mM $CaCl_2$) by rotating for 1h at 4°C. After poured into second Econocolumn, the beads were washed extensively with calmodulin binding buffer, the IRF-4-binding proteins were eluted with 1ml of calmodulin elution buffer containing 2mM EDTA instead of 2mM $CaCl_2$.

Tryptic digestion, peptide extraction, and mass spectrometric analysis

After negative-staining, the bands were excised, dehydrated in acetonitrile (WAKO, Japan) and deoxidized in DTT and ammonium carbonate buffer. Sequencing Grade Modified Trypsin (Promega) was added to each tube, and the reactions were incubated overnight at 37°C. The digested peptides were extracted from the gel with 50% acetonitrile containing 5% trifluoroacetic acid (TFA) and were dried. Tryptic peptides were sequenced by tandem mass spectrometry on a QSTAR® XL Hybrid LC/MS/MS System, hybrid quadrupole time of flight (Q-TOF) mass spectrometer (Applied Biosystems) and automated data analysis system. All of the MS/MS spectra identified from the peptide fragmentation data by the Analyst® QS software were searched against the protein sequence database maintained at the National Center for Biotechnology Information, using the MASCOT program (http://www.matrixscience.com), to identify the proteins.

Results

Identification of the proteins associated with IRF-4 by the TAP method, and subsequent mass spectrometry

To identify the proteins that associate with IRF-4 in T-cells, we purified IRF-4–binding complex by the TAP method, as described previously. Supplemental Fig.1S illustrates the purification procedures of specific binding proteins to the target TAP-tagged protein (TAP-tagged IRF-4) using two different affinity columns. The final eluates containing the IRF-4-binding protein complex (Supplemental Fig.2S-B, *EGTA*) were separated on a 4–20% SDS-PAGE gradient gel and visualized with a Negative Gel Stain MS Kit (Supplemental Fig.2S, *IRF4-TAP*). Compared to the control experiment (*WT*) using the same amount of HUT102 cells without transfection of the target TAP-tagged IRF4 expression plasmid, as many as 50 bands were stronger than the control. We excised well-separated 30 bands from the gel, digested by trypsin and identified by tandem mass spectrometry. However, only the fourteen bands in addition to IRF4 were identified with significant scores ($p < 0.05$) in the Swiss-Prot database, using the MASCOT search engine (Supplemental Table S1). One of the peptide sequences acquired from the approximately 75–80 kDa protein band was matched to the human c-Rel proto-oncogene protein with 160 Mowse score and covering 13% of the c-Rel entire 560 amino acids sequence in independent 7 peptides ($p=0.001$).

Optimization of T-cell activation with PMA, and Ionomycin, and T-cell receptor (TCR) antibodies.

We optimized the T-cell activations using EL-4 mouse T-cells, and used 250ng/ml

PMA, and 1μM Ionomycin, and plate-bound 0.5μg/ml anti-CD3, and 4μg/ml anti-CD28 for 4~8 hours to activate T cells otherwise indicated. The treatments with the same amounts of P/I, were also employed to stimulate effectively $CD4^+$ T cells, and HUT102 cells.

Figure legends

Supplemental Fig. S1 Purification scheme of IRF-4-binding proteins by the TAP strategy. The nuclear extracts prepared from cells expressing the TAP-tagged IRF-4 are subjected to two successive purification steps. The first column traps the IRF-4-TAP complex specifically, and the complex is eluted with TEV protease, leaving non-specific proteins that bind to IgG beads. The IRF-4-TAP complex binds to the second calmodulin-coated beads, to remove the TEV protease and non-specific TEV-cleaved fragments. Finally, the highly-purified IRF-4-binding complex was eluted by reducing calcium concentration with EDTA. X, Y, Z: possible IRF-4 binding protein. ●: non-specific proteins, ■: non-specific proteins that bind to IgG beads, ▼: non-specific TEV-cleaved fragments.

Supplemental Fig. S2 Actual purification of IRF-4-binding proteins by the TAP strategy.

(**A**) TAP-tagged human IRF-4 was expressed in HUT-102, an HTLV-1-infected human T cell line constitutively expressing IRF-4. The nuclear (N) and cytoplasmic (C) extracts of HUT102 cells transfected with the TAP-tagged IRF-4 expression vector (*IRF-4-TAP*) and non-transfected HUT102 cells (*WT*), were separated by 9% SDS-PAGE, blotted with an anti-IRF-4 antibody.

(**B**) Aliquot of each purification step was separated by 9% SDS-PAGE, and blotted with the anti-IRF-4 antibody to monitor the purification procedure. *Input*, input; *FT1* and *FT2*, flow through fractions from the 1st and 2nd affinity pcolumns, respectively; *TEV*, the IRF-4-TAP

complex released with TEV protease treatment; *EDTA*, the IRF-4-TAP complex eluted from the calmodulin-coated beads with EGTA.

Supplemental Fig. S3 SDS-PAGE and negative-staining of the purified IRF-4-binding proteins. The TAP-purified proteins from the extracts of cells transfected with the TAP-tagged IRF-4 expression plasmid (*IRF-4-TAP*) or non-transfected cells (*WT*), were fractionated on a 4–20% SDS-PAGE gradient gel and visualized with a negative-stain kit. About 30 protein bands were analyzed by tandem mass spectrometry (Hybrid LC/MS/MS System); the corresponding gene names identified by the MASCOT search engine (http://www.matrixscience.com), and a molecular weight marker are shown.

Supplemental Fig. S4 Optimization of T-cell activation with PMA, and Ionomycin, and T-cell receptor (TCR) antibodies. The EL-4 mouse T cells were treated with the indicated PMA, and Ionomycin, the treatment Ionomycin only or PMA for 8h, and the relative amounts of IL-2 (**A**) and IL-4 (**D**) mRNA normalized to the quantity of β-Actin mRNA were determined by real-time PCR, using the reverse-transcribed cDNAs. The IL-2 (**B**) and IL-4 (**E**) mRNA amounts relative to β-Actin mRNA were measured after the treatments of 250ng/ml PMA, and 1μM Ionomycin for the indicated time. The EL-4 T cells were stimulated with the plate-bound anti-CD3 (0.5 μg/ml) and anti-CD28 antibodies (4 μg/ml) for the indicated time, and the IL-2 (**C**) and IL-4 (**F**) mRNA amounts β-Actin mRNA were measured. The data shown are representative of three independent experiments done in triplicate.

Supplemental Table S1. Summary of the IRF-4 associating proteins.

NCBIGI#	*Protein identification*	*Protein(MW)*	*Score*[a]	*%coverage*
	Signaling intermediates			
23503048	Cleavage and polyadenylation specificity factor (CPSA)	160782	44	4
1491699	78kDa glucose-regulated protein precursor (GRP78)	72288	38	3
34978357	Heat shock 70kDa protein 6 (HSP76)	70984	79	7
123648	Heat shock 71kDa protein (HSP7C)	70854	329	27
3183544	Polyadenylate-binding protein 1 (PABP1)	70626	122	9
	Transcription regulators			
55977747	Heterogeneous nuclear ribonucleoprotein M (hnRNPM)	77333	72	5
548720	c-Rel proto-oncogene protein (c-Rel)	68476	160	13
114762	Nucleophosmin (NPM)	32555	122	13
	Ribosomal subunit			
133041	60S acidic ribosomal protein P0 (L10E)	34252	116	19
21759409	Exosome complex exonuclease RRP43	30020	77	7
133021	60S ribosomal protein L7 (RL7)	29207	52	4
	GDP/GIP binding protein			
544231	Elongation factor 1-alpha 2 (EF1A)	50438	46	2
	SDR(short-chain dehydrogenase/reductase) enzyme			
3915733	Dehydrogenase/reductase SDR family member 2 (HEP27)	27290	218	22
	Others			
57015374	Nuclear protein ZAP3	219849	133	3

The candidate proteins with significant scores ($p < 0.05$) in the Swiss-Prot database, using the MASCOT search engine are summarized.

[a]MASCOT computes the probability as a significance score, with higher scores meaning that the observed match between the experimental data and the mass values calculated from a candidate peptide or protein sequence is not a random event (http://www.matrixscience.com/).

NCBI gene identification numbers (GI#), molecular weights (MW), percentage of peptide coverage (% coverage) are also shown.

Supplemental Fig.S1

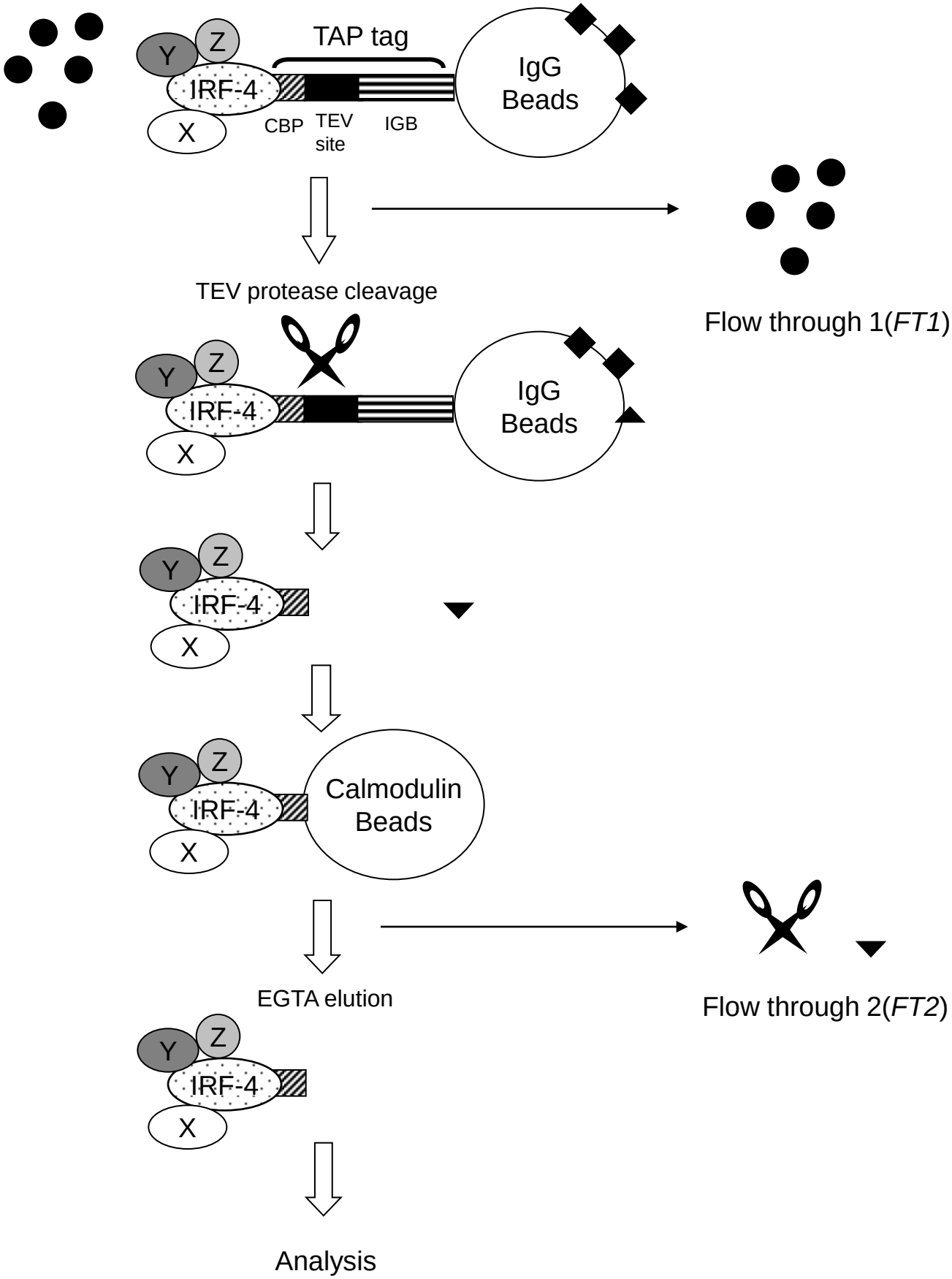

Supplemental Fig.S2

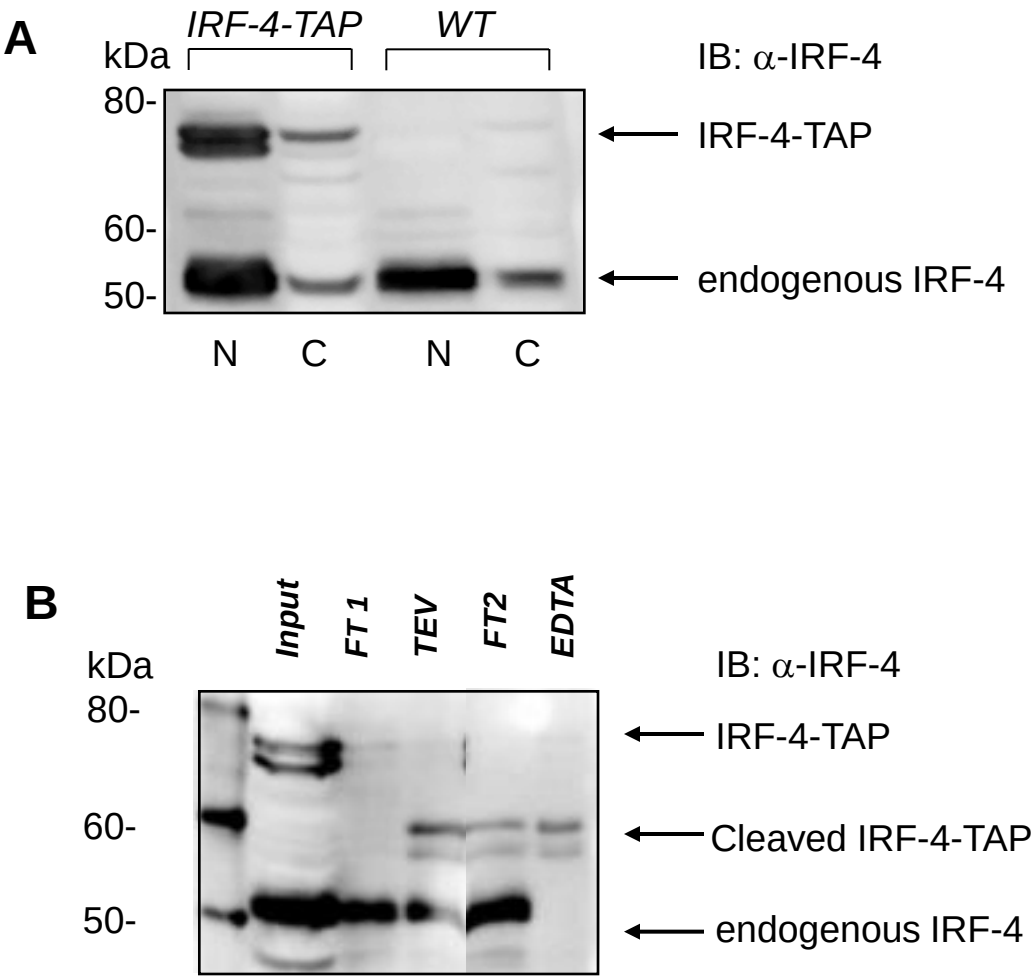

Supplemental Fig.S3

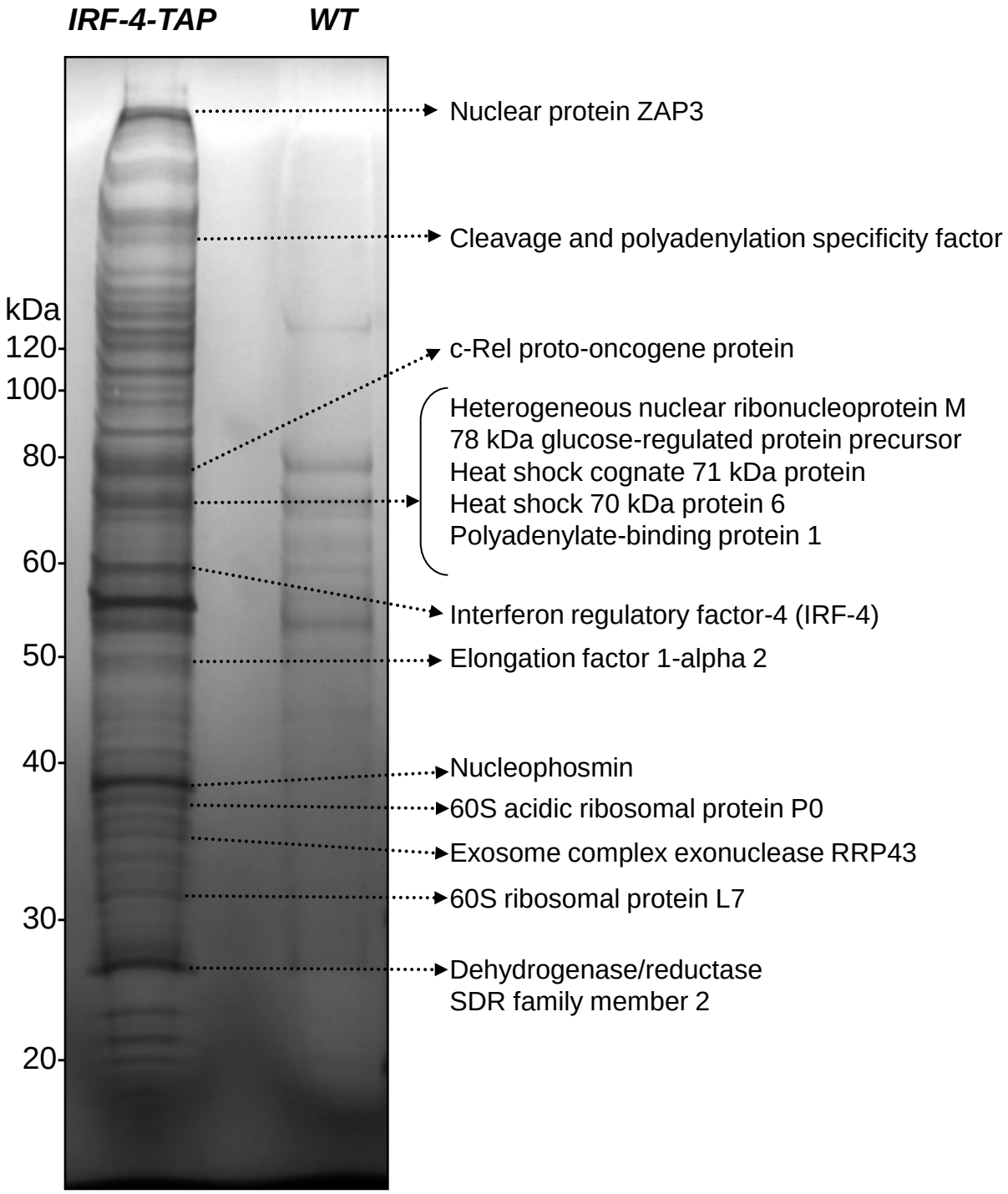

Supplemental Fig.S4